Squirrel Cage Induction Motor: A Design-Based Comparison Between Aluminium and Copper Cages

ALESSANDRO MARFOLI [1]**, MAURO DI NARDO** [1] **(Member, IEEE), MICHELE DEGANO** [1] **(Member, IEEE), CHRIS GERADA** [1]**, AND WERNER JARA** [2]

[1] Power Electronics and Machine Control Group, University of Nottingham, Nottingham NG7 2RD, U.K.
[2] Department of Electrical Engineering, Pontificia Universidad Católica de Valparaíso, Valparaíso 2340000, Chile

CORRESPONDING AUTHOR: MAURO DI NARDO (e-mail: mauro.dinardo4@nottingham.ac.uk)

ABSTRACT In many industrial applications the self-starting capability of electric motors is still an important requirement enabling to simplify the drive architecture and increase the system's reliability. The efficiency improvement of this motor topology has been targeted by various national and international regulatory authorities with ad-hoc policies. Indeed, a lower energy consumption leads to the twofold benefits of reducing the operational costs and the CO_2 emissions. The adoption of a copper cage has been successfully proven to reduce the motor losses. However, this could affect other performance indexes, such as the starting torque. In this paper, the advantages and drawbacks of adopting a copper cage are analysed in depth by comparing the motors performance at different operating conditions, with respect to the more common aluminium cage. Starting from a set of induction machines optimized with an aluminium cage, the effect of the direct material cage substitution is analysed both in terms of electromagnetic and thermal aspects. The overall performance are also compared against machines specifically optimized with a copper cage. With the presented performance comparison exercise, general design guidelines are outlined aimed at improving the efficiency without deteriorating other performance metrics.

INDEX TERMS Aluminium cage, copper cage, efficiency improvement, fast performance computation, finite element analysis, induction motor, multi-objective optimization, rotor slot design, squirrel cage.

I. INTRODUCTION

Almost 50% of the final world electric energy consumption is used to supply electric motors [1]. Although the majority of the electric motors has a rated power below 0.75 kW, it is the remaining small fraction of the overall market which has the biggest impact on the electric energy consumption, as shown in Fig. 1(b) and (c). In fact, 10% of the electric motors, the ones having power rating higher than 0.75 kW, are responsible for the 91% of the overall consumed electric energy [2]. Fig. 1(d) shows the distribution of the electric motor types in Europe divided into power ranges [3]. Clearly, the most influential motor topology in terms of electric energy consumption is the AC multi-phase one being the most common in the medium-high power range. Grid connected three phase squirrel cage induction motor (SCIM) represents the largest market share among the wide variety of AC electric motors available on the market [4]. Therefore, improving its efficiency can have the biggest effect on the reduction of the environmental impact in terms of CO_2 emissions [5]. In the last two decades, almost all the major economies have introduced some regulatory schemes (first on a voluntary basis and then mandatory), first on the minimum motor efficiency and lately on overall drive system efficiency [6]. For example in Europe, the commission regulation 1781/2019 [7] sets a precise timetable for the minimum energy efficiency requirements for electric motors both inverter and direct-grid supplied. The definition of the efficiency classes of electric motors adopted by the regulatory authorities as well as the methodology to experimentally determine the efficiency are set by the international standards IEC 60034-30-1/2 and IEC 60 034-2-1, respectively.
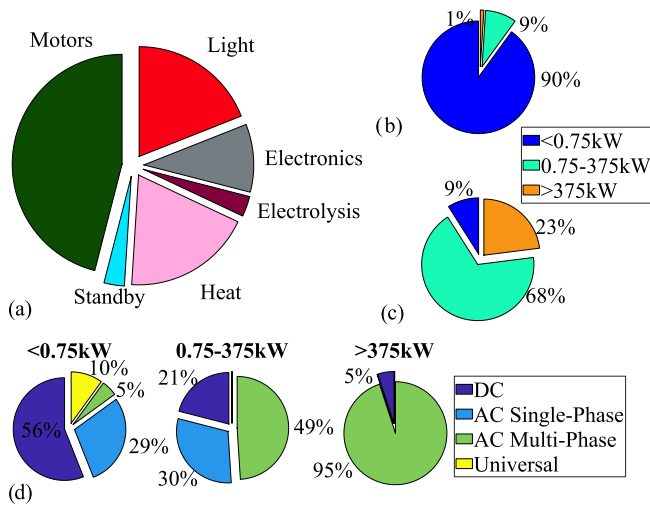
FIGURE 1. a) Electric energy consumption by end use, b) Number of motors by power range, c) Motor energy consumption by power range, d) Motor type distribution by power range.
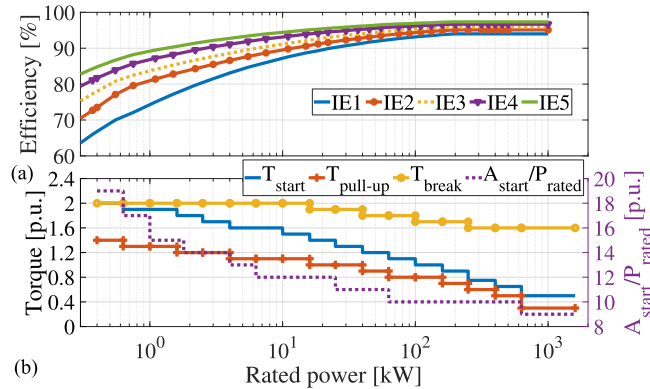

FIGURE 2. a) Efficiency levels defined by IEC 60 034-30 for a 4-poles, 50 Hz SCIM, b) Minimum torque values and locked rotor apparent power for design N defined by the IEC 60 034-12.

Along with the classification of the performance based on the energy efficiency behaviour, reported in Fig. 2(a), three phase SCIMs directly supplied by the main are subject to minimum performance requirement also in terms of torque-speed characteristics. In fact, the minimum value of the breakdown, pull-up and starting torque along with the maximum value of the starting current are specified by the IEC 60 034-12 [8] for different design types. Fig. 2(b) reports how these requirements change with the rated power. Most of the performance indexes whose boundaries are set by the mentioned standards, along with the rated power factor, are in competition, so one cannot be improved without the worsening of another. Indeed, the design of a SCIM can be considered a multi-objective optimization problem since the design choices, from the material selections to the geometric design, affect multiple competitive performance metrics. The design strategies aimed at increasing the efficiency of SCIM can be subdivided in two main families. The first one is based on modifications of existing machine's designs with the minimum economical impact for motor manufacturers, i.e. using existing stator and rotor laminations [9], [10]. Core axial lengthening, employment of better magnetic materials [11], [12] and the adoption of copper cage are some examples of this design approach. These incremental modifications of existing designs have been proved to be marginally successful to improve the efficiency, but with several limitations. In fact, a design change intended to improve the efficiency could lead to a violation of other performance indexes, such as minimum starting, pull-up and breakdown torques [13], [14]. The second option to increase the efficiency consists in a complete motor redesign. This has the advantages of achieving higher efficiency level with the best exploitation of the employed materials without compromising any other performance indexes. However, higher financial costs are expected due to the new realization or the need for a modified production line [15]. Among the several design factors affecting the SCIM performance, the shape of the slot hosting the rotor bars, plays a fundamental role in defining the torque-speed curve as well as the efficiency as a function of the load. The rotor slot design procedure usually starts from a limited set of well-known slot shapes, such as trapezoidal, rectangular, rounded or Boucherot, which can all be analytically sized [16], [17]. Given the inevitable simplifications adopted in the analytical models, a FE refinement stage is usually needed to capture the effects of small geometrical modifications [18]. An alternative approach to the design would be to use a formal optimization algorithm to determine the rotor geometry, which maximize the selected performance indexes [19], [20]. Although it can be considered a well-known and consolidated topic, the analysis and design of SCIMs, especially when carried out with the aid of optimization algorithm, still presents significant challenges because the accurate prediction of the performance requires time-consuming FEAs. Recently published work [21] have proposed a new systematic methodology to carry out the design optimization of SCIMs. An innovative mixed analytical-FEA performance evaluation method based on [22], [23] has been introduced, which is able to obtain a very fast estimation of the torque and efficiency behaviour without compromising the results' accuracy. This new performance estimation approach has been embedded within an automatic design procedure aid by stochastic optimization algorithm having the target of maximizing both starting and rated performance.

Copper rotor cages have been traditionally adopted mainly in medium-high voltage motors where pre-manufactured bars are inserted in the slot and brazed at the end-rings [24]. The recent improvement of the copper die-cast technologies has made copper cages an economically viable solution also for the small-medium power ranges where the cost of the fabricated copper bars has been the main limitation to the market acceptance [13]. Although, the replacement of the aluminium cage with copper bars has been demonstrated to be an effective methodology to improve the motor efficiency, such design modification might deteriorate the starting performance.

The aim of this paper is to quantify the effectiveness of this design solution with a systematic approach differently to

what it has been previously reported in literature. In particular, different slot shapes are considered covering a wide range of requirements in terms of starting torque and starting current.

The paper has been structured as follows. Section II briefly summarizes the rotor design optimization procedure. Section III reports the experimental tests carried out on an off-the-shelf squirrel cage induction motor with an aluminium cage in order to validate the implemented fast performance evaluation method. Section IV reports the optimization results obtained with an aluminium cage considering the motor specifications of the tested induction motor. The optimal machines producing a wide range of starting torques and rated efficiency are used as baseline designs for the subsequent comparison exercise. The effect of a straight substitution of the rotor bar material is then assessed in Section V including the thermal implications. The optimal performance of SCIMs specifically designed considering a copper cage is finally presented in Section VI. General design guidelines are finally drawn in the last section.

II. DESIGN PROCEDURE

According to the specific application, several points of the torque-speed characteristic of a SCIM can be subject to minimum requirements. The most common are the starting, the rated and the breakdown operating conditions, although sometimes particular applications may require extreme pull-up torque and minimum efficiency at partial loads. In this case study, the rated efficiency along with the starting torque have been selected to be maximized subject to a maximum value of the ratio between the starting and the rated currents.

The starting performance are calculated performing a single voltage-fed time-harmonic finite element analysis of the machine under evaluation. The rated operating point, defined as the slip in which the machine provides the rated torque, depends on the machine geometry including the rotor slot features. As a consequence, for each machine geometry evaluation, the rated slip needs to be identified. Once the performance, i.e. torque and current, corresponding to two initially supposed slips are computed, the search of the rated slip can be carried out implementing the well-known secant method. All the details of the rated slip identification are fully described in [21], including a strategy to reduce the iterations required to find the rated operating point. The performance for each slip are calculated solving the single phase equivalent circuit featuring lumped parameters determined with time-harmonic finite element simulations (TH-FEA). Among the existing methods aimed at determining the SCIM equivalent circuit parameters from TH-FEAs, the one reported in [22] has been adopted given its improved accuracy even when evaluating closed rotor slot geometries. In order to avoid characterizing each parameters for the entire current range, an iterative method has been proposed in [21]. At every iteration the current computed solving the equivalent circuit is compared with the one used in the TH-FEA and when an acceptable error between these values is reached, the steady state performance for the simulated slip is determined. Fig. 3 summarizes
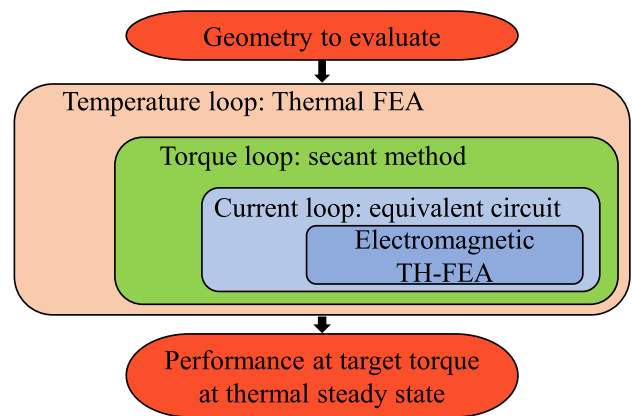
FIGURE 3. Flow chart of the iterative procedure for the evaluation of the machine performance for a given torque.
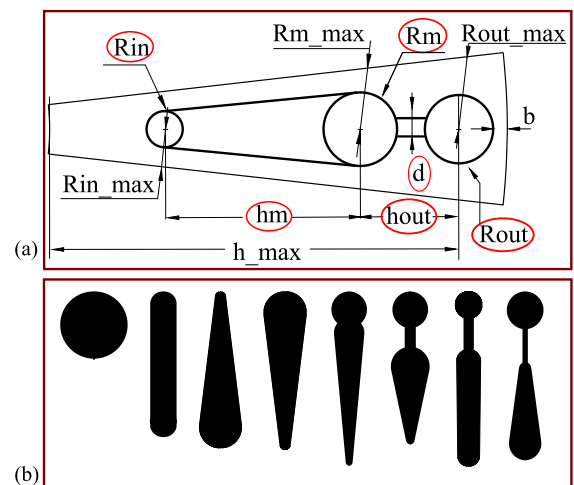
FIGURE 4. a) Rotor slot parametrization, b) examples of slot shapes investigated during the optimization.

the flowchart of the overall performance estimation method. The external thermal-FE loop aimed at identifying the steady state temperatures of both stator and rotor windings is not enabled during the optimization, but it is used only during the post-processing re-evaluation of the optimal machines. By doing so, the computational cost is greatly reduced without affecting the accuracy of the optimization results, as will be shown in the next sections.

The geometrical variables to be identified during the rotor design are circled in red in Fig. 4a. The adopted per unit parametrization allows drawing and therefore investigating all the possible symmetric variants of single and double rotor slots (Fig. 4b reports some samples of the possible geometries explored).

A stochastic multi-objective optimization algorithm (NSGA-II embedded in Matlab) with a population size of 60 elements evolving for 60 generations is used to identify the six rotor geometrical variables while the stator geometry is kept constant. Table 1 reports the main geometrical parameters and specifications of the baseline machine.

TABLE 1. Baseline Machine Specifications and Parameters

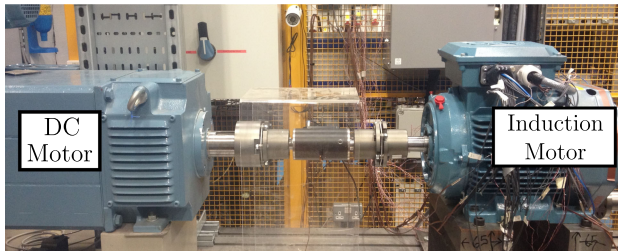| Parameter	Value	Unit
Rated torque	75	Nm
Rated frequency	50	Hz
Rated voltage	400	V
Number of poles	4	n.d.
Number of stator slots	36	n.d.
Number of rotor bars	28	n.d.

FIGURE 5. Experimental test rig layout.

III. EXPERIMENTAL VALIDATION OF THE PERFORMANCE EVALUATION METHOD

The performance of an off-the-shelf SCIM are computed with the methodology detailed in Section II and compared against the experimental test results. The main characteristics and geometrical parameters of the motor under test are reported in Table 1. The aim of this paragraph is to asses the accuracy of the performance evaluation approach used throughout the presented in depth analysis. The experimental test rig consists in the SCIM under test connected to a speed-controlled DC motor via a torque transducer as shown in Fig. 5. Thermocouples has been placed in the end windings of the motor in order to measure the temperature of the coils on both drive-end and not-drive-end of the motor. For every operating point the input and output powers have been measured with the torque sensor and the power analyser to identify the electromagnetic steady state performance of the motor under test. Fig. 6(a)–(d) show a comparison between the experimental and the predicted results in per unit in terms of torque, stator current, power factor and efficiency. The compared quantities show a good agreement, thus confirming the accuracy of the adopted performance evaluation approach and consequently the validity of the comparison exercises between aluminium and copper cages. Fig. 6(e) shows the thermal transient to achieve the steady state winding temperature when the motor generates the rated torque. Operating points above the rated slip value (overload conditions) has been tested quickly to avoid over-heating of the motor.

IV. OPTIMAL ALUMINIUM CAGE RESULTS

The rated efficiencies and the starting torques of the most performing SCIMs with an aluminium cage is shown in Fig. 7(a). These results are obtained from 3 of the most significant optimizations, considering three different values of maximum current ratios ($kI = 5.4/7.4/n.d.$ where the $n.d.$ stands for not defined). The coefficient kI is as the ratio between
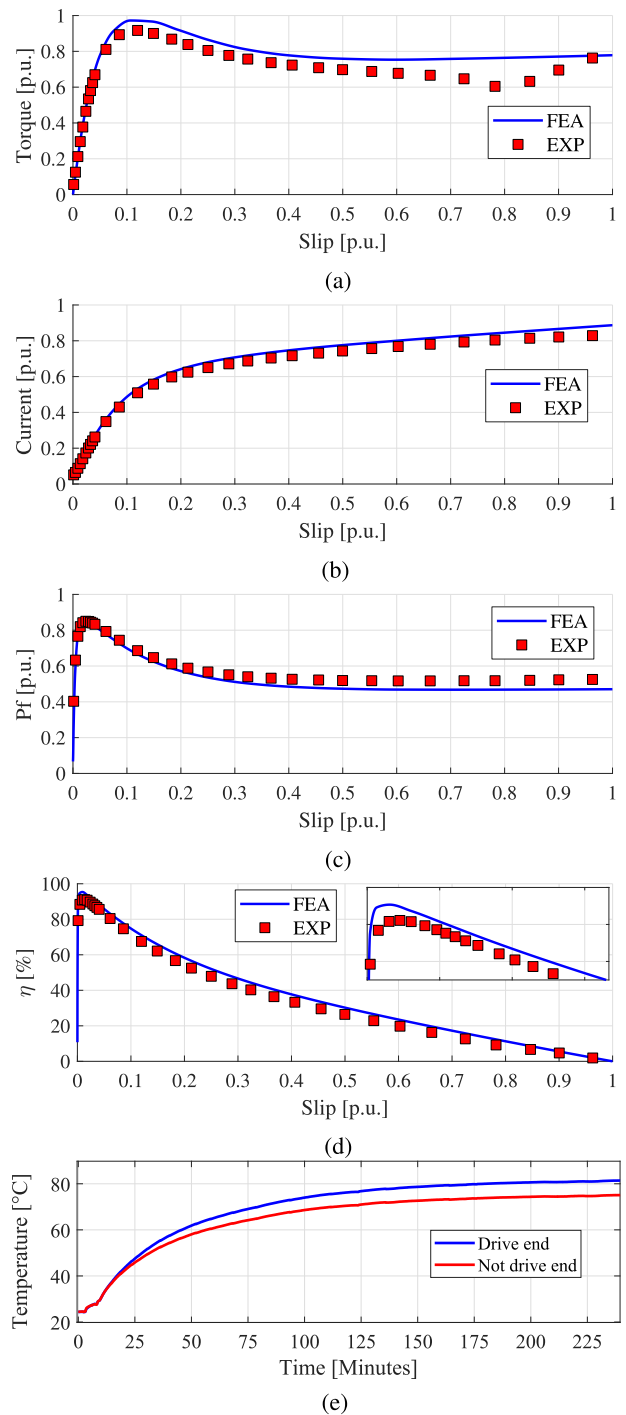

FIGURE 6. Comparison between measured and estimated torque (a), stator current (b), power factor (c) and efficiency (d). Winding temperatures at the rated operating condition from cold to thermal steady state.

starting and rated currents. It can be noticed that the range of variation of the starting torque is much bigger than the rated efficiency one. Relaxing the starting current limit permits to achieve higher rated efficiency. However, as kI increases the efficiency gain reduces and it becomes null for designs featuring high starting torques. As expected, the rotor slot surface (shown in Fig. 7b) increases as the rated efficiency increases.
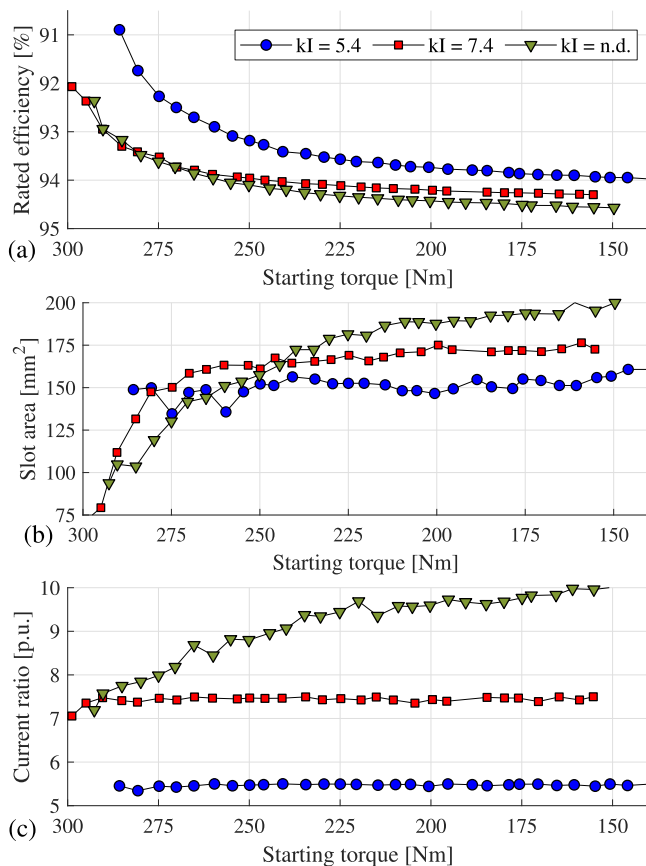
FIGURE 7. a) Optimized performance of the aluminium rotor cage for three different maximum current ratios *kI*; b) rotor slot area and current ratio c) of the optimal geometries.

In fact, on the one hand, small slots feature higher starting resistance and so high starting torque. On the other hand, bigger slots allows for a lower rated resistance and so a higher rated efficiency. The relaxation of the current ratio constraint allows bigger slot surfaces which in turns leads to designs with higher rated efficiency for a given starting torque. The last statement holds only in the low-medium starting torque range. In fact, for designs producing high starting torques, increasing the current ratio limit allows achieving the same rated efficiency but with a lower slot area. Fig. 7 c) shows the ratio between starting and rated currents. When the current ratio is constrained, the effective current ratio always reaches the imposed boundary. On the contrary, when unlimited, it increases with the rated efficiency.

Fig. 8 shows a subset of optimal rotor slots for three different *kI*. Along with the slot surface, the most influencing geometrical parameter upon the performance indexes is the neck length (*hout*). Increasing the distance between the outer and inner cages has the twofold effect of 1) emphasising the non-uniform current density distribution at the starting condition, leading to an enhanced starting torque due to the higher starting resistance and 2) increasing the rated leakage reactance that worsen the rated efficiency, rated power factor and breakdown torque. The above considerations are endorsed
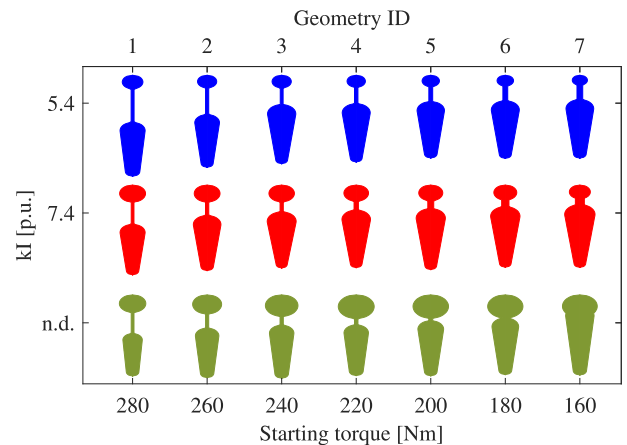

FIGURE 8. Optimal rotor slot geometries with an aluminium cage.
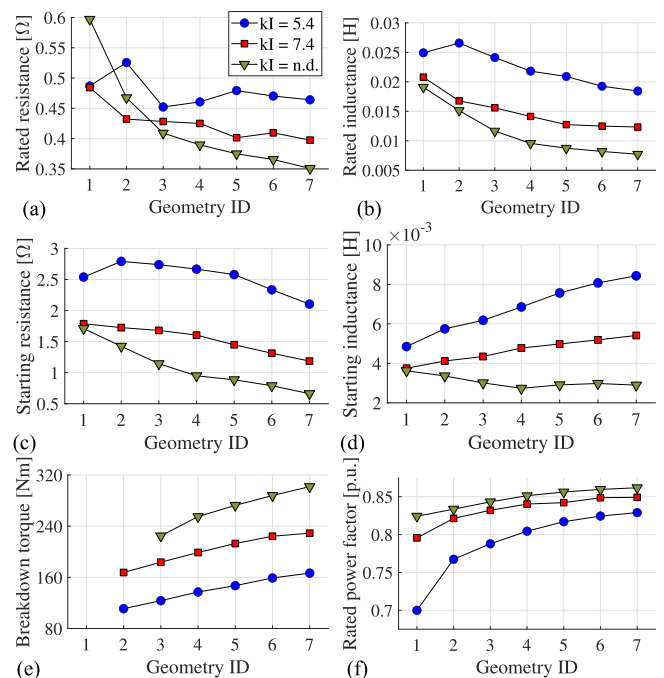

FIGURE 9. Rotor resistance and leakage inductance at the rated (a, b) and starting conditions (c, d) of the optimal aluminium cage solutions along with the breakdown torque (e) and rated power factor (f).

by Fig. 9, which shows the rotor resistance and leakage inductance at the rated and starting conditions along with the breakdown torque and rated power factor.

As previously mentioned, the rotor slot optimization is carried out considering constant stator and rotor windings temperatures (T-Win, T-Cage), respectively to 80 and 100 °*C*. It is reasonable to expect that when the performance are re-evaluated at thermal steady state, the rated efficiency will change. In particular, machine designs with higher losses will experience bigger efficiency variations.

Fig. 10 confirms the above statements being the efficiency variation higher for lower current ratio limits and so for less efficient designs (which clearly have a higher temperature rise). From the same figure, it is also possible to note that such
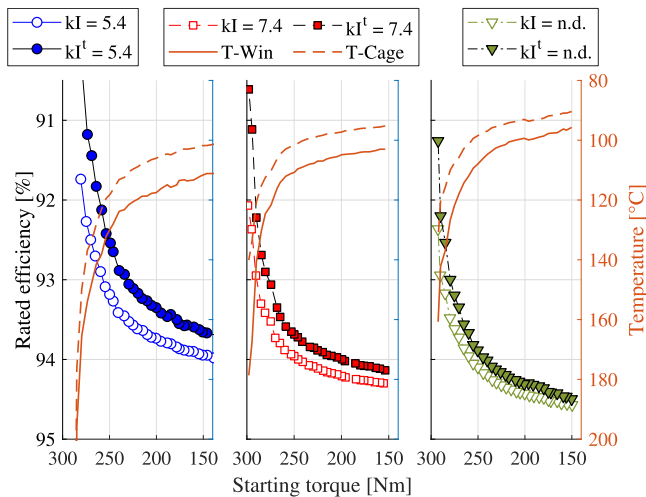
FIGURE 10. Comparison between the rated efficiencies calculated with constant windings temperature (*kI*) and re-evaluated at the correct temperature (*kI^t*); the steady state temperatures of stator and rotor windings (*T − Win*, *T − Cage*) are also reported.

efficiency gap is almost constant for a given current ratio limit. This justifies the choice of optimizing the rotor slot geometry neglecting the thermal aspect since when considered it does not invalidate the optimality of the results.

V. STRAIGHT SUBSTITUTION OF ALUMINIUM WITH COPPER

A common design practice to improve the rated efficiency is the direct substitution of the rotor cage material passing from aluminium to copper. The effects of such substitution on all performance indexes are not fully investigated and reported in literature and this paragraph attempts to fill this gap. In the following, this replacement is applied to the designs optimized for an aluminium cage shown in Fig. 8 featuring a vast range of performance in terms of starting torque, rated efficiency and current ratio. Fig. 11 summarizes the percentage variations of all performance considered when copper is used with respect to the performance of the baseline optimal aluminium rotor designs. Analysing these trends the following considerations can be drawn.

- No matter which machine is considered, i.e. for any current limit considered and starting torque produced, the copper cage always improves the rated efficiency as shown in row *a*) of Fig. 11. The efficiency gain is in the range 0.5-1.25% and it is bigger for baseline machines with low efficiency, i.e. the ones with high starting torques and low *kI*. In other words, the most efficient baseline SCIM experiences the lowest efficiency improvement (0.5%).

- The same graphs in the first row also report the efficiency gain when considering the same stator and rotor winding temperatures for both material cages (dotted black lines). Clearly a relevant portion (20-40%) of the efficiency gain is due to the lower temperatures experienced by the machines with the copper cage, as shown in row *b*).

The remaining efficiency improvement quota is ascribed to the lower copper resistivity and so lower rated rotor resistance, as shown in row *c*) of the figure.

- As expected the efficiency improvement is mainly due to the lower rotor joule losses as depicted in row *d*), although also the stator joule losses decreases as a consequence of the lower stator winding temperature (the rated current remains unchanged).

- Interesting to notice that the power factor do not change as the ratio between the rotor resistance and the slip and the leakage inductance remain constant as shown in row *e*).

- Unfortunately, the efficiency enhancement comes at the price of the violation of the starting current limit, as shown in row *f*). The starting to rated current ratio increment lies in the range 0-25% and it tends to be proportional to the efficiency gain.

- Unexpectedly, the starting torque does not always deteriorate when substituting the aluminium cage with the copper one, as depicted in Fig. 11*f*). In particular, for low current ratio designs (*kI* = 5.4), the starting torque always increases while for high current ratio (*kI* = n.d.) the starting torque always decreases. In the middle range, i.e. *kI* = 7.4, the starting torque variation sign depends on the considered baseline design, being negative for high starting torque baseline designs and positive for lower ones.

- Although unexpected, this phenomenon can be physically explained by looking at resistance and leakage inductance variations at the starting condition, shown in row *g*). At the starting operating point the change of material determines a more intensified skin effect, as shown in row *l*), which reports the relative variation of the current density distributions. This is due to the relation between current density and electric field $J = \sigma E$ and it is more significant for machines with high IDs. As a consequence, the starting resistance reduction, due to the higher copper conductibility, is not equal for all the designs, but it decreases as the starting torque of the baseline machine decreases. At the same time, the more disuniform current distributions also causes a reduction of the leakage inductance (see row *g*)). Although, the lower resistance should reduce the starting torque, the decrement of the leakage inductance increase the starting current and in some cases this leads to a higher starting torque with respect to the aluminium cage.

- In row *h*), it is worth noting that the material cage substitution does not affect the breakdown torque but it does decrease the relative slip of about 35%. This is clearly due to the fact that the breakdown resistance decreases, while the leakage inductance does not, as reported in row *i*).

VI. OPTIMAL COPPER CAGE RESULTS

The optimal aluminium cage (*Al*) along with the results of the straight substitution of the aluminium with the copper
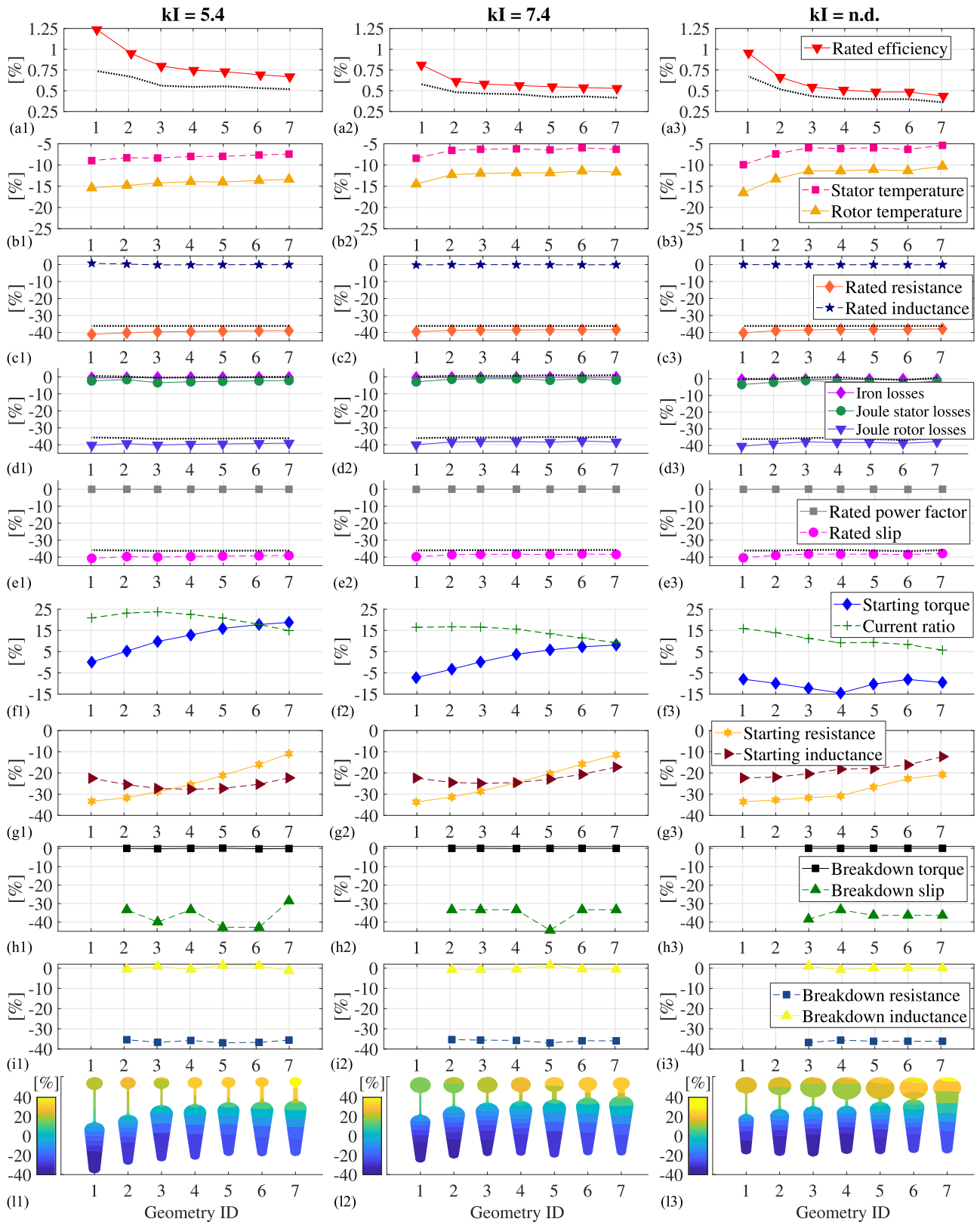
FIGURE 11. Performance and rotor parameters variations when directly replacing the aluminium cage with the copper one: a) Rated efficiency at the same temperature and new steady state temperature, b) stator and rotor temperatures, c) rated resistance and inductance, d) iron and joule losses, e) power factor and rated slip value, f) starting torque and current ration *kI*, g) resistance and inductance at the starting operating point, h) breakdown torque and slip, i) breakdown resistance and inductance and l) variation of the current density distribution.
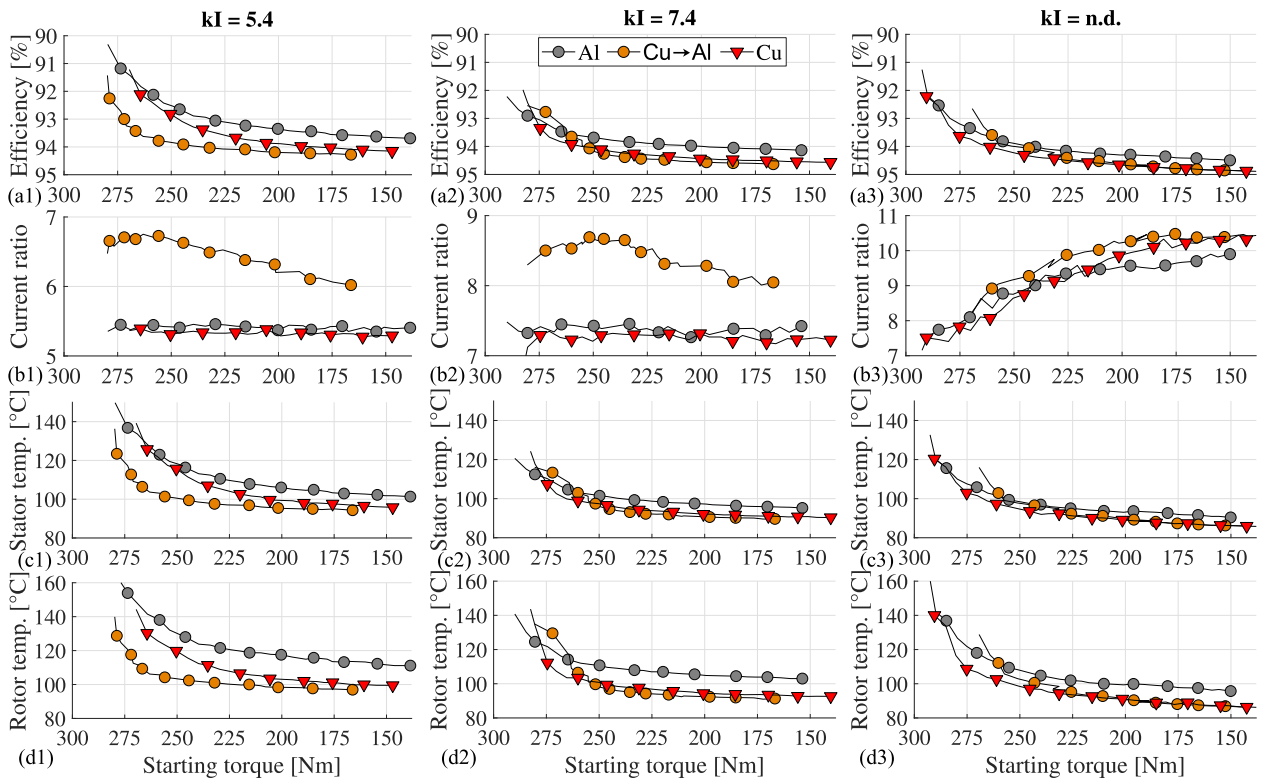
FIGURE 12. Rated efficiency (a), effective current ratio (b), stator (c) and rotor (d) winding temperatures as function of the starting torque for machines optimized with the aluminium (*Al*) and the copper (*Cu*) cage along with the straight substitution of the material cage (*Cu → Al*).

($Cu \rightarrow Al$) are hereafter compared with the optimal copper rotor cage (*Cu*). This comparison is deemed to be a very interesting exercise in order to evaluate the benefits of the copper cage adoption according to how the latter is implemented. In the following, different optimization results are reported for the three maximum current ratios *kI* already defined for the aluminium cage. Fig. 12 reports the main performance indexes selected to compare the three series of designs. The first row *a*) shows the starting torque and rated efficiency calculated at thermal steady state. The second row *b*) reports the effective current ratios of the optimum motor designs while the stator winding and rotor cage temperatures at rated operating point are compared in the last two row *c*) and *d*). Analysing these results the following consideration can be done.

- The copper cage obtained either from straight substitution or through optimized design exhibit a higher efficiency with respect to the aluminium cage. This is true whatever design is considered in terms of starting torque and current ratio.
- The optimized copper cages present the same range of starting torques provided by the aluminum rotor cage but with a higher rated efficiency. The efficiency improvement is higher for low-medium starting torques and becomes negligible for very high starting torque values.
- The motor featuring optimized copper cage provides an improved efficiency performance with respect to the straight copper replacement only when the constraint of the maximum current ratio is completely released. For

low values of *kI*, the straight substitution of aluminium with copper allows achieving a higher efficiency with respect to the optimized copper cage. However, this comes at the cost of a higher starting to rated current ratio (as shown in Fig. 12(b)).

- Although the copper cage has been optimized considering the same maximum current ratios, the optimal copper designs provides the same starting capability of the optimal aluminium cage with a higher rated efficiency.
- Stator and rotor temperatures at the rated operating point reported in row *c*) and *d*) feature similar trends of the rated efficiencies. Lower stator windings and cage temperatures are experienced by motors featuring copper cages thanks to the lower losses.

Fig. 13(a) reports the cross section areas of the bars as well as the ratio between the upper cage area and the total bar area. The resistance and reactance of the optimal solutions at the rated and starting operating points are depicted in Fig. 13(b) and (c), respectively. In Fig. 14 the optimal aluminium and copper bar shape are shown along with the current density distribution at locked rotor condition. Analysing these figures the following conclusion are drawn.

- In general, the optimum copper and aluminium cages exhibit a quite similar bar shape with some small differences.
- The optimum aluminium cages feature a bar cross section area bigger than the copper cage one. This is due to the different resistivity that leads to reduce the
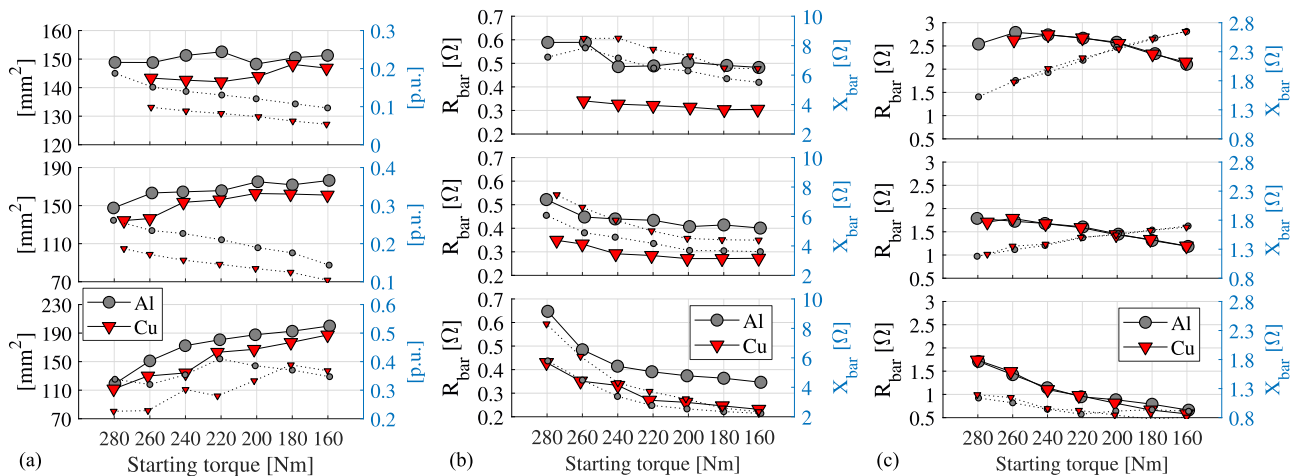
FIGURE 13. Optimal aluminium and copper a) slot area and ratio between outer and inner cage area (dotted lines), b) rated rotor resistance and reactance (dotted lines), c) starting resistance and reactance (dotted lines). First row corresponds to the lowest maximum current ratio $k_I = 5.4$ while for the third row $k_I = n.d.$.
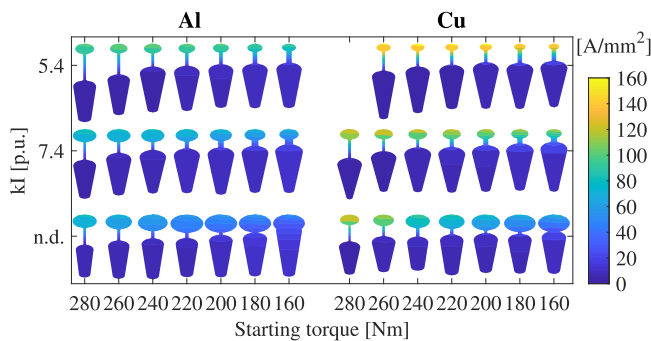

FIGURE 14. Current density distribution of the optimal aluminium and copper cage designs.

copper bar section to satisfy the same starting requirements.

- In fact, given a certain current ratio and starting torque, the same starting rotor impedance (Fig. 13(c)) is achieved by the copper bar lowering the ratio between upper and total cross section area with respect to the aluminium cage. In other words, the optimal copper bar features a lower overall area with a bigger portion dedicated to the inner cage being smaller the outer one. This is an additional source of efficiency improvement. This lower bar head dimension is clearly needed to enhance the skin effect phenomenon, as depicted in Fig. 14.

- The effect of the different shape of the copper and aluminium bars is reflected in Fig. 13(b) where the rotor parameters are compared at rated operating point. Although, the copper cage features a geometry that enhance the rated reactance (always higher than the aluminium cage), the efficiency of the copper solution is still higher than the aluminium one, thanks to the lower resistance. In other words, the lower resistance of the copper cage guarantees a better efficiency also with a bar shape that increase the leakage inductance.

It is worth to underline that some of the obtained optimal rotor slot geometries might be at the limit of the manufacturability (for certain cutting and die casting process) given the small thickness of the connecting slit between the outer and inner cages. This is particularly evident for rotor slots providing the highest starting torque where the optimization algorithm has pushed the connecting slit dimensions at the imposed boundaries in order to increase the starting leakage inductance. The definition of a minimum thickness of the rotor slot has to be selected according to the requirements of the cutting and die cast manufacturing processes. In the reported case study, the considered minimum slot dimension is 0.5 mm, corresponding to the thickness of the rotor slot bridge (*b* in Fig. 4(a). Such value can definitely impact on the optimum rotor bar shape and therefore on the performance. For instance, an increment of this minimum value would provide optimum solutions featuring deeper bar shapes in order to satisfy extreme starting requirements and consequently have lower rated efficiency.

VII. CONCLUSION
The presented work compares different squirrel cage induction motors featuring aluminium and copper cages. Based on the findings highlighted in the previous sections, the most salient conclusions are drawn as follows.

- The straight substitution of the aluminium with the copper leads to a higher efficiency at the cost of a higher starting current.
- The direct replacement of the cage material causes the starting torque increment for baseline designs with low starting currents. Conversely, the starting torque worsen when considering baseline designs with high starting current.
- An optimized rotor copper bar allows to obtain a better efficiency with respect to the optimal aluminium solution without exceeding the starting current limit with a reduction of the slot area (less conductive material).

- The smaller outer cage dimensions of the optimal copper solutions allows reaching the same starting performance of the aluminium cage, while the lower copper resistivity along with the bigger inner cage cross section cause the rated efficiency improvement.

For the analysed machine, the efficiency improvement achieved adopting an optimal copper cage lies in a tight range of about 0.5-1%, where the higher gains are related to less efficient baseline design/application (requiring high starting torque) whilst lower gains are achieved with the best performing baseline designs. Instead, the straight material cage substitution allows achieving similar efficiency gain of a customized design (except for low k_I) with the disadvantages of substantially increasing the starting current and/or using more conductive material. The marginal efficiency improvement of the copper cage with respect to the aluminium ones imposes the adoption of accurate but fast analysis and design tool, as the one proposed in this manuscript, in order to highlight the several design trade-offs and avoid selecting sub-optimal designs.

ACKNOWLEDGMENT

REFERENCES

[1] P. Waide and C. Brunner, "Energy-efficiency policy opportunities for electric motor-driven systems," in *IEA Energy Papers, No. 2011/07, OECD Publishing, Paris*, 2011. [Online]. Available: https://doi.org/10.1787/5kgg52gb9gjd-en

[2] de Almeida, H. Falkner, A. C. João Fong, and K. Jugdoyal, "Eup Lot 30: Electric motors and drives. Final Report for the European Commission," Institute of Systems and Robotics, Univ. of Coimbra, 2014.

[3] A. Almeida, J. Fong, H. Falkner, and P. Fonseca, "From laggard to world leader - the role of policies in the EU motors and drives market transformation," in *Proc. Eur. Council Energy Efficient Economy*, 2015, pp. 1549–1557.

[4] A. T. De Almeida, F. J. T. E. Ferreira, and A. Q. Duarte, "Technical and economical considerations on super high-efficiency three-phase motors," *IEEE Trans. Ind. Appl.*, vol 50, no. 2, pp. 1274–1285, Mar./Apr. 2014.

[5] A. T. de Almeida, P.Fonseca, and P. Bertoldi, "Energy-efficient motor systems in the industrial and in the services sectors in the european union: Characterisation, potentials, barriers and policies," *Energy*, vol. 28, no. 7, pp. 673–690, 2003.

[6] L. Alberti and D. Troncon, "Design of electric motors and power drive systems according to efficiency standards," *IEEE Trans. Ind. Electron.*, to be published, doi: 10.1109/TIE.2020.3020028.

[7] Official Journal of the European Union "COMMISSION REGULATION (EU) 2019/1781 of 1 October 2019," [Online]. Available: https://eur-ex.europa.eu/eli/reg/2019/1781/oj

[8] Rotating Electrical Machines—Part 12: Starting Performance of Single Speed, Three Phase, Cage Induction Motor, Int. Std. IEC/EN 60034-12, 2016.

[9] A. Boglietti, A. Cavagnino, L. Ferraris, M. Lazzari, and G. Luparia, "No tooling cost process for induction motors energy efficiency improvements," *IEEE Trans. Ind. Appl.*, vol. 41, no. 3, pp. 808–816, May 2005.

[10] E. B. Agamloh, A. Boglietti, and A. Cavagnino, "The incremental design efficiency improvement of commercially manufactured induction motors," *IEEE Trans. Ind. Appl.*, vol. 49, no. 6, pp. 2496–2504, Nov. 2013.

[11] L. Alberti, N. Bianchi, A. Boglietti, and A. Cavagnino, "Core axial lengthening as effective solution to improve the induction motor efficiency classes," *IEEE Trans. Ind. Appl.*, vol. 50, no. 1, pp. 218–225, Jan. 2014.

[12] F. Parasiliti, "Design strategies, new materials and technologies to improve induction motors efficiency," *Prace Instytutu Elektrotechniki, Z.* vol. 223, pp. 27–42, 2005.

[13] F. Parasiliti and M. Villani, "Design of high efficiency induction motors with die-casting copper rotors," *Energy Efficiency Motor Driven Syst.,* vol. 1, pp. 144–151, 2003.

[14] C. G. Heo, H. M. Kim, and G. S. Park, "A design of rotor bar inclination in squirrel cage induction motor," *IEEE Trans. Magn.*, vol. 53, no. 11, pp. 1–4, Nov. 2017.

[15] A. Cavagnino, S. Vaschetto, L. Ferraris, Z. Gmyrek, E. B. Agamloh, and G. Bramerdorfer, "Striving for the highest efficiency class with minimal impact for induction motor manufacturers," *IEEE Trans. Ind. Appl.*, vol. 56, no. 1, pp. 194–204, Jan./Feb. 2020.

[16] I. Boldea and S. A. Nasar, *The Induction Machines Design Handbook. Electric Power Engineering Series*. CRC Press/Taylor & Francis, 2010.

[17] T. A. Lipo, *Introduction to AC Machine Design*. IEEE Press Series on Power Engineering, Wiley, 2017.

[18] A. C. Smith, "Integrating FE into induction motor design-a marriage of inconvenience?," in *Proc. IEE Seminar Curr. Trends Use Finite Elements (FE) Electromechanical Des. Anal.* (Ref. No 2000/013), pp. 4/ 1–4/7, Jan. 2000.

[19] S. Williamson and C. I. McClay, "Optimization of the geometry of closed rotor slots for cage induction motors," *IEEE Trans. Ind. Appl.*, vol. 32, no. 3, pp. 560–568, May 1996.

[20] G. Lee, S. Min, and J. Hong, "Optimal shape design of rotor slot in squirrel-cage induction motor considering torque characteristics," *IEEE Trans. Magn.*, vol. 49, no. 5, pp. 2197–2200, May 2013.

[21] A. Marfoli, M. Di Nardo, M. Degano, C. Gerada, and W. Chen, "Rotor design optimization of squirrel cage induction motor - Part I: Problem statement," *IEEE Trans. Energy Convers.*, to be published, doi: 10.1109/TEC.2020.3019934.

[22] D. Genovese, P. Bolognesi, M. De Martin, and F. Luise, "A contextual parameter identification method for the equivalent circuit of induction machine," in *Proc. 22th Int. Conf. Elect. Machines*, Sep. 2016, pp. 25–31.

[23] A. Marfoli, L. Papini, P. Bolognesi, D. Genovese, and C. Gerada, "Analysis of induction machine: Comparison of modelling techniques," in *Proc. IEEE Int. Electric Machines Drives Conf.*, May 2017, pp. 1–7.

[24] W. R. Finley and M. M. Hodowanec, "Selection of copper versus aluminum rotors for induction motors," *IEEE Trans. Ind. Appl.*, vol. 37, no. 6, pp. 1563–1573, Nov. 2001.

ALESSANDRO MARFOLI received the M.Sc. degree in electrical engineering from the University of Pisa, Pisa, Italy, in 2015 and the Ph.D. degree in electrical machine design from the University of Nottingham, Nottingham, U.K., in 2020. He is currently a Research Fellow within the same institution working on wide variety of projects of high industrial and scientific impacts. His main research focuses on the modelling, analysis and optimization of electrical machines including induction and synchronous machines also for bearingless applications.

MAURO DI NARDO (Member, IEEE) received the M.Sc. (Hons.) degree in electrical engineering from the Polytechnic University of Bari, Bari, Italy, in 2012 and the Ph.D. degree in electrical machine design from the University of Nottingham, Nottingham, U.K., in 2017. From 2017 to 2019, he was the Head of AROL Research Team within the Polytechnic University of Bari leading industrial R&D projects on electrical drives design for mechatronics applications. Since 2019, he has been with Power Electronics and Machine Control Group, University of Nottingham, as a Research Fellow. His research focuses on the analysis, modelling, and optimizations of electrical machines, including permanent magnet and synchronous reluctance topologies for automotive, aerospace sectors, and induction motor for industrial applications.

MICHELE DEGANO (Member, IEEE) received the master's degree in electrical engineering from the University of Trieste, Trieste, Italy, in 2011, and the Ph.D. degree in industrial engineering from the University of Padova, Padua, Italy, in 2015. Between 2014 and 2016, he was a Postdoctoral Researcher with The University of Nottingham, Nottingham, U.K., where he joined the Power Electronics, Machines and Control Research Group. In 2016, he was appointed Assistant Professor of advanced electrical machines with The University of Nottingham. In 2020, he was promoted as an Associate Professor. His main research focuses on electrical machines and drives for industrial, automotive, railway and aerospace applications, ranging from small to large power. He is currently the PEMC Director of Industrial Liaison leading research projects for the development of future hybrid electric aerospace platforms and electric transports.

CHRIS GERADA received the Ph.D. degree in numerical modeling of electrical machines from The University of Nottingham, Nottingham, U.K., in 2005.

He was a Researcher with The University of Nottingham, working on high-performance electrical drives and on the design and modeling of electromagnetic actuators for aerospace applications. Since 2006, he has been the Project Manager of the GE Aviation Strategic Partnership. In 2008, he became a Lecturer of electrical machines, in 2011, as an Associate Professor, and in 2013, a Professor with The University of Nottingham. His main research focuses on the design and modeling of high-performance electric drives and machines.

Prof. Gerada is an Associate Editor for the IEEE TRANSACTIONS ON INDUSTRY APPLICATIONS and he is also the Chair of the IEEE Industrial Electronic Society Electrical Machines Committee.

WERNER JARA received the B.Sc. degree in electrical engineering from the University of Concepción, Concepción, Chile, in 2010, the dual D.Sc. degree from the University of Concepción, Concepción, Chile, and the Lappeenranta University of Technology, Lappeenranta, Finland, in 2016. He is currently a Lecturer with the Department of Electrical Engineering, Pontificia Universidad Católica de Valparaíso, Valparaíso, Chile. His current research interests include the field of electrical machines and drives, particularly numerical modeling, and design of electromagnetic devices.